

# Influence of cyclophilin D protein expression level on endothelial cell oxidative damage resistance

J.Z. Peng<sup>1</sup>, L. Xue<sup>2</sup>, J. Chen<sup>3</sup>, B.S. Chen<sup>1</sup> and Y.Q. Yang<sup>3</sup>

<sup>1</sup>Department of Cardiothoracic Surgery,  
The Third Affiliated Hospital of South Medical University, Guangzhou, China

<sup>2</sup>Red Cross Hospital of Guangzhou, Guangzhou, China

<sup>3</sup>Department of Cardiothoracic Surgery,  
The Second Affiliated Hospital of Sun Yat-Sen University, Guangzhou, China

Corresponding author: Y.Q. Yang

E-mail: pjzh\_one@163.com

Genet. Mol. Res. 14 (2): 4258-4268 (2015)

Received May 30, 2014

Accepted October 29, 2014

Published April 28, 2015

DOI <http://dx.doi.org/10.4238/2015.April.28.7>

**ABSTRACT.** We examined the influence of cyclophilin-D (CypD) protein expression level on endothelial cell oxidative damage resistance. A model of CypD protein expression or high expression in endothelial cells was established through gene silencing or cloning. The comparable groups were normal endothelial cells cultured in phosphate-buffered solution in liquid handling cells containing 500  $\mu\text{M}$   $\text{H}_2\text{O}_2$  for 90 or 120 min, and then the medium was replaced with common nutrient solution and cultured again for 24 h. The apoptosis rate and nitric oxide (NO) levels of each group were tested. The cell apoptosis rate of the CypD low expression group ( $32.51 \pm 6.6\%$ ) was significantly lower than that of the control group ( $52.57 \pm 5.84\%$ ,  $P = 0.001$ ), and total NO production was  $24.06 \pm 3$  and  $13.03 \pm 3.55$   $\mu\text{M}$ . The apoptosis rate of the CypD high expression group ( $24.24 \pm 3.08\%$ ) was significantly higher than that of the control group ( $7.7 \pm 0.68\%$ ,  $P < 0.001$ ); total NO production was  $3.55 \pm 1.53$  and  $8.46 \pm 0.77$   $\mu\text{M}$ , which was significantly different

( $P = 0.008$ ). CypD protein could increase oxidative stress and cause endothelial cell injury and apoptosis.

**Key words:** Cyclophilin-D protein; Endothelial cells; Oxidative stress

## INTRODUCTION

As a member of the cyclophilins family, cyclophilin-D (CypD) protein possesses peptidyl-proline cis-trans isomerase (PPIase) activity. CypD protein, located in the mitochondrial matrix, is a component of the mitochondrial permeability transition pore (MPTP). One way in which the mitochondria react to oxidative stress and sulfur preparations is by combining adenine nucleotide translocator (ANT) and free CypD proteins to increase the sensitivity of MPTP on calcium ions (Halestrap, 1999; Vyssokikh et al., 2001; Lummis et al., 2005). Under the stimulation of various injury factors, calcium ion concentration is increased in cells. Through the transduction of the calcium signal, CypD protein in the mitochondrial matrix, together with voltage-dependent ion channels and ANT, forms a composite material, resulting in the formation and opening of an adjustable MPTP. The mitochondrial matrix begins to swell and the intimal potential declines, initiating depolarization of intimal, outer mitochondrial membrane ruptures, and cytochrome C and apoptosis-inducing factor and some stromal proteins are released, ultimately leading to cell death (Wang, 2001; Scorrano et al., 2002).

A previous study found that during myocardial ischemia reperfusion injury, MPTP opening during ischemia is not obvious, but significant opening can be observed during reperfusion. Thus, myocardial recovery depends on whether the subsequent MPTP is closed (Halestrap et al., 1998). This may be because of conditional changes after ischemia reperfusion, such as accumulation of reactive oxygen species (ROS), pH normalization, and calcium concentration increase, all of which create an ideal environment for MPTP opening (Di Lisa and Bernadi, 2006). In the high-heat specific CypD protein expression mouse model established by Baines et al. (2005), large amounts of cytochrome C were released in the myocardium, caspase 9 and myocardial apoptosis increased, and the heart became larger, while cardiac function significantly decreased. Upon disruption of the interaction between CypD protein and ANT or when CypD protein and ANT ectopic expression occurred, resistance to apoptosis was observed (Temkin et al., 2006). Thus, reducing factors that induce MPTP opening can protect the myocardium from being injured during myocardial reperfusion (Javadov et al., 2003; Halestrap et al., 2004; Argaud et al., 2005). Gene knockout technology was used to establish CypD protein deficiency model rats. Upon death of the rats resulting from myocardial infarction, the area of myocardial infarction had decreased by nearly 40% compared with that of normal rats under the same conditions. In addition, CypD protein deficiency-type mitochondria could also resist the calcium ion induced by the release of cytochrome C relatively better than the normal mitochondria (Baines et al., 2005).

Vascular endothelial cells are the first line of defense against various stress factors. Nearly all known risk factors causing coronary heart disease are associated with endothelial dysfunction (De Meyer and Herman, 1997; Woodman et al., 2003). However, the relationship between CypD protein and vascular endothelial cell function, as well as the occurrence and function in the development of CypD protein in atherosclerosis and stenosis, remain unclear.

## MATERIAL AND METHODS

The human umbilical vein endothelial cell line ECV304 was purchased from the Center of Wuhan University (Wuhan, China). High-sugar Dulbecco's modified Eagle medium (DMEM) and fetal bovine serum were from Gibco (Grand Island, NY, USA). The 30% H<sub>2</sub>O<sub>2</sub> was from Sigma (St. Louis, MO, USA). Anti-cyclophilin D antibody was from Bioreagents Company (Bio-Tek, Beijing, China). The Annexin V-FITC kit was from Bender MedSystems (Vienna, Austria). Lipofectamine 2000 was from Invitrogen (Carlsbad, CA, USA). Small interfering RNA (siRNA) was from Shang Gemma Biotechnology (Toronto, Canada). Peptidylprolyl isomerase F (*ppif*) cDNA was from Guangzhou Lederer Biotechnology Co. Ltd. (Guangzhou, China). The total nitrogen oxide detection kit was from Bi Yuntian Biological Technology Institution (Shanghai, China). A Nikon eclipse TE2000-U fluorescence microscope was used (Tokyo, Japan). For transmission electron microscopy, a Hitachi H-7500 transmission electron microscope was used (Hitachi, Tokyo, Japan). The FA Sort flow cytometry instrument was from BD Biosciences (Franklin Lakes, NJ, USA). The CELL Quest software was used for analysis (BD Biosciences). A Rotor-Gene 6000 Real-Time PCR machine was used (Qiagen, Hilden, Germany).

An endothelial cell apoptosis model was established by inoculating ECV304 cells on 6-well plates at  $1 \times 10^6$  cells per well; wells were randomly divided into 4 groups (A, B, C, D), with each three replicates per group. After the cells had grown and adhered to 90%, we used phosphate-buffered saline (PBS) with 100, 300, and 500  $\mu$ M H<sub>2</sub>O<sub>2</sub>, respectively, and cultured ECV304 cells at saturation humidity, 37°C, 5% CO<sub>2</sub> for 0, 30, 60, 90, and 120 min. The PBS containing H<sub>2</sub>O<sub>2</sub> was removed and PBS was used to wash the cells 3 times until the H<sub>2</sub>O<sub>2</sub> was removed. High-sugar DMEM containing 10% fetal bovine serum was added to the culture medium and the cells were cultured for 24 h; group D was used as the blank control group. After washing the cells as described above, we used fluorescence correlation microscopy to detect the cell apoptosis rate. The oxidative stress concentration showing the best compliance was used to establish the endothelial cell apoptosis model.

Changes in H<sub>2</sub>O<sub>2</sub>-induced endothelial cell apoptosis and CypD protein expression level were determined using the apoptosis model. We detected changes in stress time of CypD protein expression levels as well as cell oxidative stress. Total RNA was extracted and we detected the changes in stress time of *ppif* gene expression level along with cell oxidative stress.

To establish a model for downregulated CypD expression, ECV304 cells were inoculated on 6-well plates at  $1 \times 10^6$  cells/well; after 24 h, when cells had reached 80% confluence, according to manufacturer recommendations, Lipofectamine 2000 was used to transfect siRNA against the *ppif* gene into ECV304 cells. After 6 h, a fluorescence microscope and flow cytometer were used to test the transfection efficiency. Common medium was used to culture the cells for an additional 12, 24, 48, and 72 h. Quantitative reverse transcription-polymerase chain reaction (qRT-PCR) was used to detect the efficiency of *ppif* silencing, and western blot analysis was used to detect CypD protein expression. In the CypD downregulated group, siRNA was used to target the *ppif* mRNA: sense 5'-G CCGCUUCCUGACGAGAATT-3' and anti-sense 5'-UUCUCGUCAGGAAAGCGGCTT-3'.

The time at the highest rate of silencing was used as the down-regulated CypD model group, which was compared with normal cells (2 groups of cells were placed in an oxidative stress environment to induce apoptosis for 120 min). H<sub>2</sub>O<sub>2</sub> and necrotic cells were removed using sterile PBS and the medium was replaced with high-sugar DMEM containing 10% fetal

bovine serum medium, followed by incubation for 24 h. The rate of apoptosis was detected in the 2 groups by fluorescence correlation microscopy and by measuring the nitric oxide content in the culture medium. Ultrastructure changes in the cells were observed in both groups by transmission electron microscopy.

To establish a model for upregulated CypD expression, *ppif*-cDNA synthesized by Guangzhou Lederer Company was inoculated into cells on five 6-well plates at  $1 \times 10^6$  cells per well and shaken well. After the cells reached 80% confluence, cell samples were collected at 0, 12, 24, 48, and 72 h (repeated 3 times for each time point). qRT-PCR and western blot detection were used to determine when CypD expression was highest.

Cells showing upregulation of CypD expression were compared with normal cells; the 2 groups of cells were placed in an oxidative stress environment required for the apoptosis model for 90 min.  $H_2O_2$  and necrotic cells were removed using sterile PBS and replaced with high-sugar DMEM containing 10% fetal bovine serum for 24 h. Apoptosis was detected in both groups by fluorescence correlation microscopy and by measuring nitric oxide content in the culture medium.

For statistical analysis, the measurement data showing a normal distribution are reported as means  $\pm$  SD; the SPSS16.0 software was used for analysis of variance (SPSS, Inc., Chicago, IL, USA) to compare means between groups. Bivariate correlation analysis was also conducted and the means of the values were determined. When  $\alpha = 0.05$  or  $P < 0.05$ , the difference was regarded as statistically significant.

## RESULTS

### Influence of different concentrations of $H_2O_2$ on ECV304 cell apoptosis

Changes in the apoptosis rate in ECV304 cells for each group at different time points are shown in Table 1. Analysis of variance between groups revealed that the cell apoptosis rate in groups A, B, and D were not significantly different ( $P > 0.05$ ), but the difference between group C and groups A, B, and D were statistically significant ( $P < 0.01$ ). The differences at each point of time for group C were statistically significant ( $P < 0.05$ ). Pearson correlation analysis revealed that the apoptosis rate in group C was significantly and positively correlated with  $H_2O_2$  exposure time ( $r = 0.982$ ,  $P < 0.001$ ).

**Table 1.** Changes in the ECV304 apoptosis rate after  $H_2O_2$  or PBS treatment at different times. Apoptosis rate in each group (% , means  $\pm$  SD ).

Group	0 min	30 min	60 min	90 min	120 min
A <sup>a</sup>	3.52 $\pm$ 1.16	3.18 $\pm$ 2.5	6.05 $\pm$ 2.42	6.97 $\pm$ 0.52	5.22 $\pm$ 0.6
B <sup>b</sup>	3.06 $\pm$ 2.12	4.62 $\pm$ 3.93	9.67 $\pm$ 0.74	8.29 $\pm$ 0.41	9.56 $\pm$ 2.77
C <sup>c</sup>	3.66 $\pm$ 1.51	14.04 $\pm$ 0.65 <sup>d</sup>	20.67 $\pm$ 2.62 <sup>d</sup>	35.09 $\pm$ 4.45 <sup>d</sup>	47.14 $\pm$ 11.06 <sup>d</sup>
D	3.41 $\pm$ 0.8	7.12 $\pm$ 1.55	4.78 $\pm$ 0.31	8.1 $\pm$ 2.32	7.41 $\pm$ 2.42

<sup>a</sup>Compared with the D group,  $P = 0.17$ ; <sup>b</sup>compared with group D,  $P = 0.072$ ; <sup>c</sup>with A, B, D group,  $P = 0.001$ ; <sup>d</sup>comparison with 0 min,  $P < 0.05$

### Time-dependent changes in CypD protein expression under conditions of endothelial cell oxidative stress

The results of CypD-protein electrophoresis are shown in Figure 1. The Bandscan 5.0 software was used to visualize the bands; the gray value ratio (C/ $\beta$  value) of CypD and  $\beta$ -actin

was used to standardize CypD protein expression. With increased time of exposure to oxidative stress, the luminance of CypD protein bands strengthened gradually. Bivariate correlation analysis revealed that the C/ $\beta$  ratio, the time of action of  $H_2O_2$ , and the cell apoptosis rate were significantly positively correlated ( $r = 0.967$ ,  $P < 0.001$  and  $r = 0.971$ ,  $P < 0.001$ ). Time-dependent changes in *ppif* mRNA expression in ECV304 cells in the presence of  $500 \mu M H_2O_2$  are shown in Figure 2. The differences in *ppif* expression at each point of time compared to controls were statistically significant ( $P < 0.05$ ).

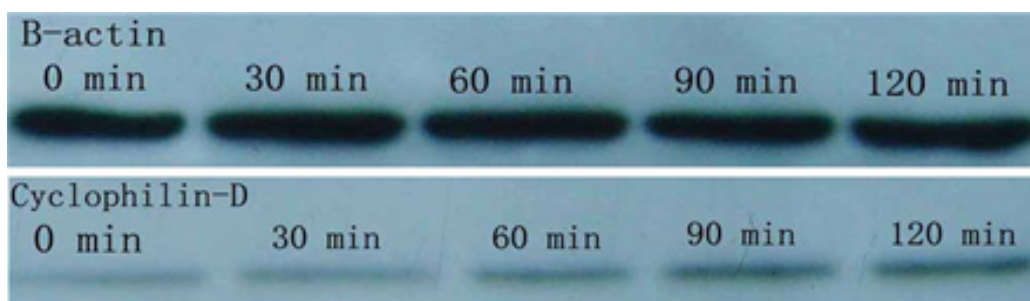


**Figure 1.** Cyclophilin D protein electrophoresis. Upper: electrophoregram of  $\beta$ -actin cytoskeleton protein electrophoresis. Lower: CypD protein electrophoresis. With increased oxidative stress time, the CypD protein expression level increased gradually.

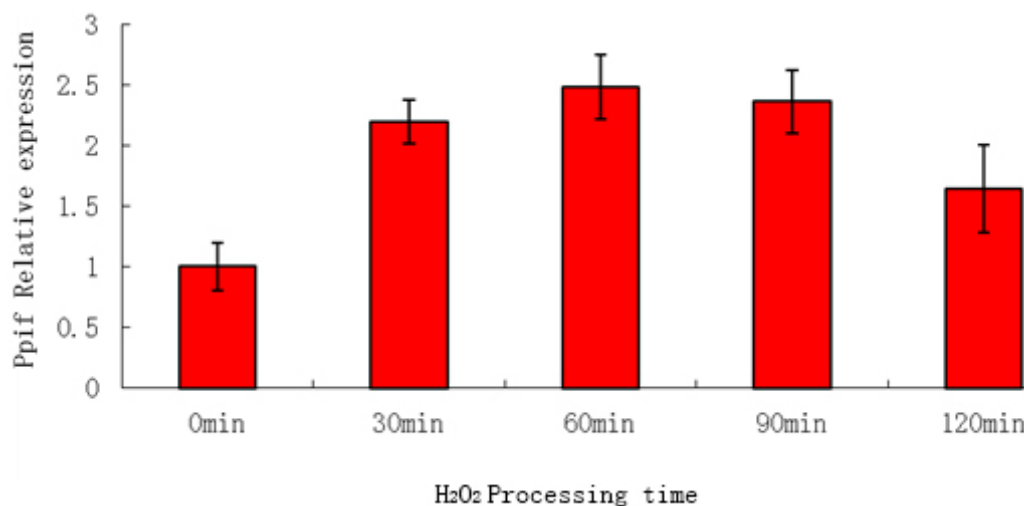


**Figure 2.** Group C *ppif* relative gene expression at each time point. After treatment of cells with  $500 \mu M H_2O_2$ , *ppif* mRNA expression levels changed over time. Compared with 0 min, *ppif* mRNA expression increased over time, reaching a maximum at 60 min.

Treatment of cells with  $500 \mu M H_2O_2$  altered the relative mRNA expression level of *ppif*. Compared to 0 min, the relative expression levels of *ppif* mRNA at each point of time increased, reaching a maximum at 60 min.

The effects of siRNA transfection are shown in Figure 3. The overall transfection rate was  $97.96 \pm 0.31\%$ . qRT-PCR results showed that after transfection, *ppif* silencing reached

a maximum at 48 h, as shown in Figure 4. Western blot analysis showed that CypD protein expression decreased with a longer transfection time, as shown in Figure 5.

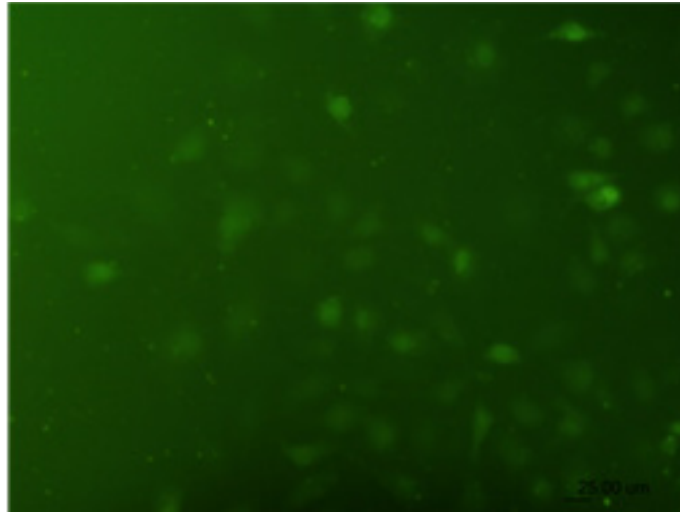


**Figure 3.** siRNA ECV304 cells after transfection for 6 h (with fluorescence controlled sequence by Lipofectamine2000 FAM - siRNA - transfection reagent mixed transfection). Fluorescence microscopy magnification 200X.

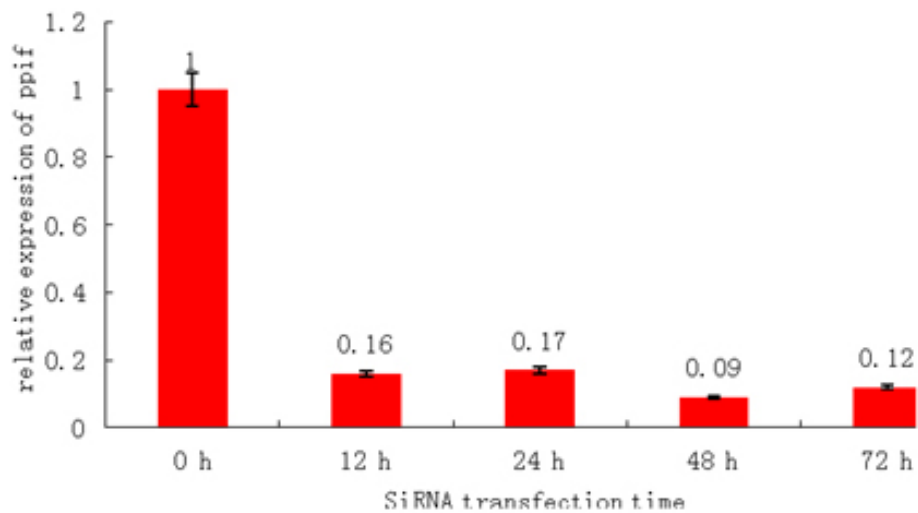


**Figure 4.** siRNA *ppif* silencing efficiency (for reference).



**Figure 5.** siRNA after transfection, CypD protein expression changes over time.

Cells showing downregulation of CypD after siRNA treatment for 48 were used as the model group and compared with normal cells under oxidative stress conditions. The apoptosis rates of the 2 groups were  $32.51 \pm 6.6$  and  $52.57 \pm 5.84\%$ , respectively, and the difference was statistically significant ( $P = 0.001$ ). Two independent samples *t*-tests showed that the total nitric oxide content in the cell culture was significantly different between the 2 groups. Nitric oxide production in the CypD downregulation group was significantly higher than that in normal cells ( $P = 0.015$ ) (Table 2).

**Table 2.** Nitric oxide production in two groups of cells treated with  $500 \mu\text{M H}_2\text{O}_2$ .

	Normal cell control group	CypD protein reduction group	P
Total amount of nitric oxide (mM)	$13.03 \pm 3.55$	$24.06 \pm 3$	0.015

Transmission electron microscopy was used to compare the blank control group with normal cells that rarely showed apoptosis (no oxidative stress treatment) (Figure 6a and b). ECV304 cells in the control group showed significant changes in apoptosis rate, as observed by the large numbers of apoptotic cells, decreasing cell microvilli, and broken nuclei fragmentation. Typical nuclear chromatin concentration was observed and distributed in the surrounding of the nuclear membrane. The mitochondria were highly swollen, organelles were highly disruptive and contained a larger number of vacuoles, some of the shapes of cells were indistinguishable. (Figure 6c and d). In the downregulated CypD group, the number of apoptotic cells was significantly lower than that in the control group. There were also fewer morphological changes, more features of early apoptosis, mitochondrial swelling into a ball shape, part of the cavity, the cell membrane was still normal (Figure 6e and f).

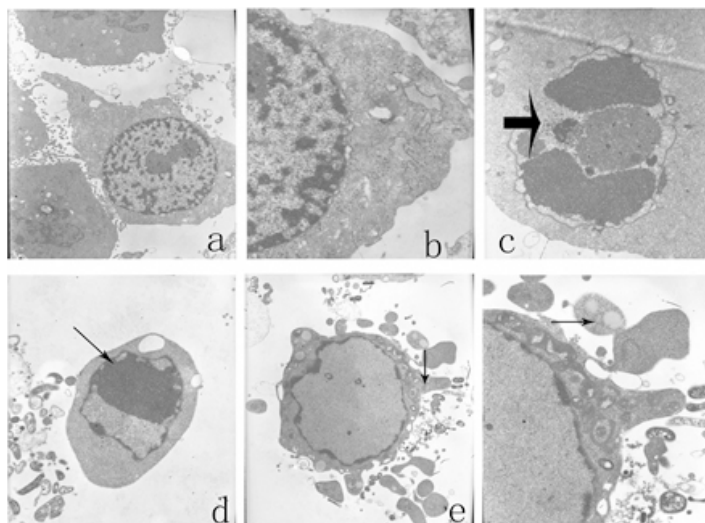


**Figure 6.** Ultrastructure and apoptosis of cells. **a. b.** Normal ECV304 cells (a: 3900X; b: 11,500X); **c. d.** Apoptotic cells in the control group (c: 8900X, a typical nuclear pyknosis, splitting into 3 large pieces; d: 6610X, a typical nuclear pyknosis thick poly edge set); **e. f.** CypD downregulated group the apoptosis of cells, mitochondria swelling into a ball shape, part of the cavity, the cell membrane was still normal (e: 520X; f: 11,500X).

For the CypD upregulated group, primer sequences used to amplify the *ppif* mRNA were: 5'-TTTAAGCTTATGCTGGCGCTGCGCTGCGGCTCCCGCTGG-3' (*Hind*III); (*ppif*-r): 5'-GCGAATTCCAGCTCAACTGGCCAC-3' (*Eco*RI). The compound *ppif* cDNA sequence is: ATGCTGGCGCTGCGCTGCGGCTCCCGCTGGCTCGGCCTGCTCTC-CGTCCCGCGCTCCGTGCCGCTGCGCCTCCCGCGGGCCCGCGCCTGCAG-CAAGGGTCCGGCGACCCGTCTTCTCTCTCTCTCCGGGAACCCGCTCGT-GTACCTGGACGTGGACGCCAACGGGAAGCCGCTCGGCCGCGTGGTGCTG-GAGCTGAAGGCAGATGTCGTCCCAAAGACAGCTGAGAAGTTCAGAGCCCT-GTGCCTGGTGAGAAGGGCTTCGGCTACAAAGGCTCCACCTTCCACAGGGT-GATCCCTTCTTTCATGTGCCAGGCGGGCGACTTCACCAACCACAATGGCA-CAGGCGGGAAGTCCATCTACGGAAGCCGCTTTCCTGACGAGAAGTTCAC-TACTG6AAGCACGTGGGGCCAGGTGTCTGTCCATGGCTAATGCTGGTCCTA-ACACCAACGGCTCCCAGTTCTTCATATGCACCATAAAGACAGACTGGTTG-GATGGCAAGCATGTTGTGTTTCGGTCAAGTCAAAGAGGGCATGGACGTCGT-GAAGAAAATAGAATCTTTCGGCTCTAAGAGTGGGAGGACATCCAAGAAGATT-GTCATCACAGACTGTGGCCAGTTGAGCTG. The results showed that the genetic homology of the synthetic *ppif* cDNA sequence and human endothelial cell *ppif* was 99%, gaps = 0/622 (0%).

Time-dependent changes in CypD protein expression after *ppif* transfection in cells are shown in Figure 7. Transfection of the *ppif* plasmid increased CypD cell protein expression with increasing transfection time, peaking at 48 h. After treatment with 500  $\mu$ M H<sub>2</sub>O<sub>2</sub>, the independent sample *t*-test was used to detect the difference in the apoptosis rate between the upregulated CypD expression and the control group (Table 3). The results showed that the apoptosis rates of the up-regulated CypD expression group was significantly higher than that in the control group cells ( $P < 0.001$ ). Total nitric oxide content in the cell culture of the upregulated CypD group was significantly lower than that in the control group ( $P = 0.008$ ) (Table 4).

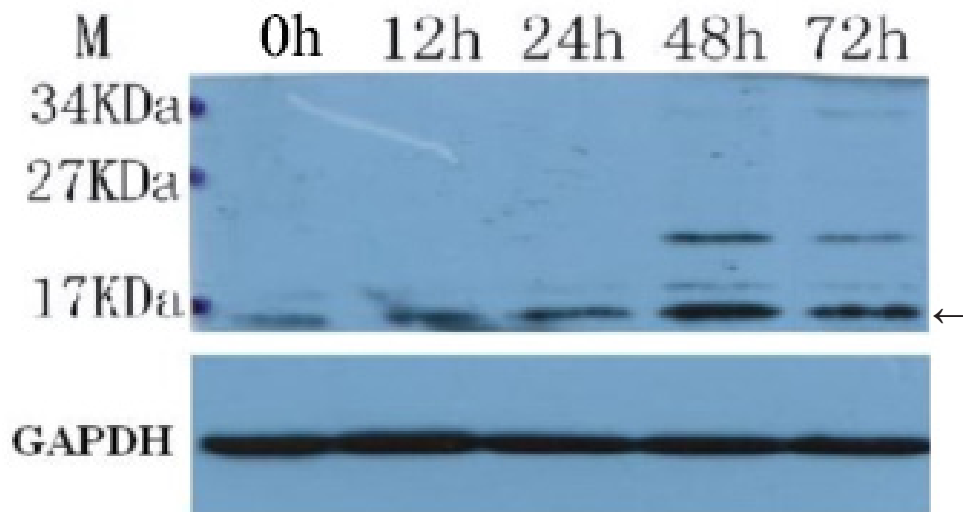


**Figure 7.** Changes in CypD protein expression from *ppif* plasmid over time. Note: the arrow is the CypD protein bands. This figure shows that with increased transfection time, CypD protein expression increased, peaking at 48 h.

**Table 3.** Apoptosis rate in the 2 groups of cells after 500- $\mu\text{M}$   $\text{H}_2\text{O}_2$  treatment.

	Normal cell control group	<i>ppif</i> plasmid transfection group	P
Apoptosis rate (%)	7.7 $\pm$ 0.68	24.24 $\pm$ 3.08	<0.001

**Table 4.** Nitric oxide production in the 2 groups of cells after 500- $\mu\text{M}$   $\text{H}_2\text{O}_2$  treatment.

	Normal cell control group	CypD high expression group	P
Total amount of nitric oxide ( $\mu\text{M}$ )	8.46 $\pm$ 0.77	3.55 $\pm$ 1.53	0.008

Analysis of time-dependent changes in CypD protein expression after *ppif* transfection revealed an extended transfection time (Figure 8). CypD protein expression continually increased, peaking at 48 h.

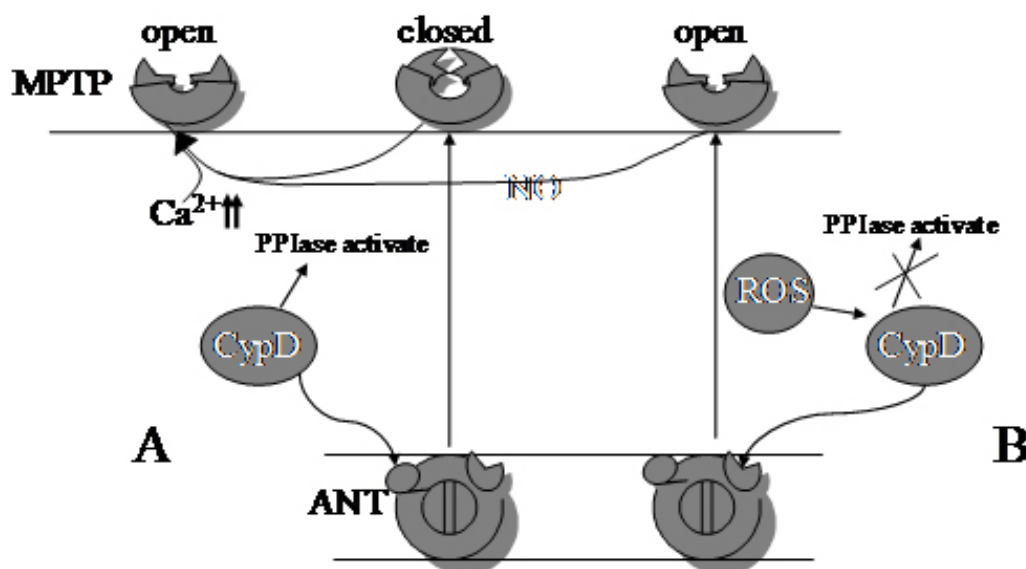


**Figure 8.** Two types of MPTP structures. **A.** Structure with PPIase activity; CypD combined with ANT resulting in closure of MPTP; **B.** Structure with lost CypD PPIase activity; CypD and ANT move to another site after combining, resulting in MPTP opening.

## DISCUSSION

Cyclophilin proteins are a family of highly conserved intracellular proteins, whose core sequences are nearly identical with those of the PPIase enzyme. They are commonly found in the biological world, and their functions include immune suppression, viral infection, molecular chaperones, cell death (apoptosis/necrosis), and optical transmission.

In this study, we observed that with extended oxidative stress time, endothelial cell apoptosis gradually increased and its intracellular mitochondria CypD protein and encoding gene *ppif* relative expression levels also gradually increased. Therefore, a clear relationship exists between oxidative stress, mitochondrial CypD protein expression, and endothelial cell

apoptosis, and CypD proteins may bridge oxidative stress and endothelial cell apoptosis.

We further established downregulated and upregulated CypD protein expression endothelial cell models. Through gene silencing or overexpression, we used H<sub>2</sub>O<sub>2</sub> to cause oxidative damage and thus induce apoptosis, and then compared the reaction with that of normal endothelial cells under oxidative stress conditions. The results suggested that under oxidative stress condition, CypD protein is the key factor in ROS-induced mitochondrial damage, further leading to apoptosis of endothelial cells (Figure 9) (Halestrap et al., 1998; Hursting et al., 2002; Baines et al., 2005; Nakagawa et al., 2005; Yasuda et al., 2006). We speculated that the molecular mechanism may increase ROS, so that CypD loses PPIase enzyme activity, while increased ROS may also increase CypD protein expression without PPIase activity through some unknown signal transduction pathways. Combined with ANT, ROS promotes the opening of MPTP, further damaging cells.

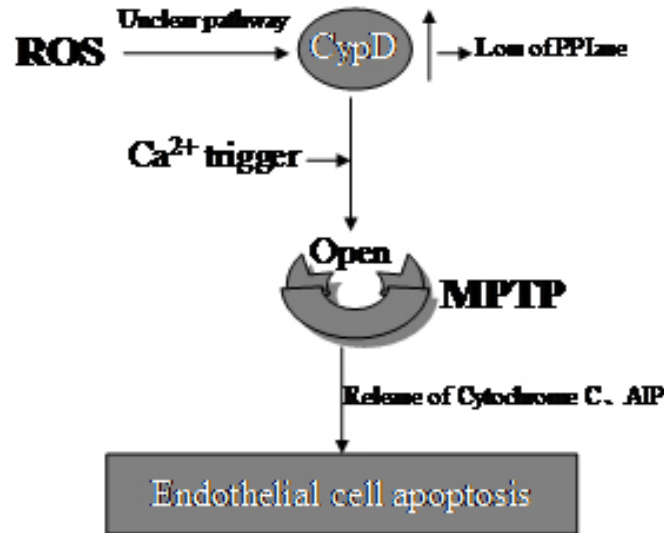


**Figure 9.** Increased ROS induced CypD induced by endothelial cell apoptosis (AIP, apoptosis inducing protein).

Further in-depth studies of ROS, CypD protein, and the relationship between endothelial cell functions are necessary. Studies should be conducted to examine the role of ROS in the increase in CypD protein. Animal experiments will increase the understanding of endothelial dysfunction and a variety of cardiovascular diseases, providing a theoretical basis for clinical prevention and treatment of these diseases.

## REFERENCES

- Argaud L, Gateau-Roesch O, Muntean D, Chalabreysse L, et al. (2005). Specific inhibition of the mitochondrial permeability transition prevents lethal reperfusion injury. *J. Mol. Cell Cardiol.* 38: 367-374.
- Baines CP, Kaiser RA, Purcell NH and Blair NS (2005). Loss of cyclophilin D reveals a critical role for mitochondrial permeability transition in cell death. *Nature* 434: 658-662.
- De Meyer GR and Herman AG (1997). Vascular endothelial dysfunction. *Prog Cardiovasc. Dis.* 39: 325-342.
- Di Lisa F and Bernardi P (2006). Mitochondria and ischemia-reperfusion injury of the heart: fixing a hole. *Cardiovasc. Res.* 70: 191-199.

- Halestrap AP (1999). The mitochondrial permeability transition: its molecular mechanism and role in reperfusion injury. *Biochem. Soc. Symp.* 66: 181-203.
- Halestrap AP, Kerr PM, Javadov S and Woodfield KY (1998). Elucidating the molecular mechanism of the permeability transition pore and its role in reperfusion injury of the heart. *Biochim. Biophys. Acta* 1366: 79-94.
- Halestrap AP, Clarke SJ and Javadov SA (2004). Mitochondrial permeability transition pore opening during myocardial reperfusion - a target for cardioprotection. *Cardiovasc. Res.* 61: 372-385.
- Hursting SD, Shen JC, Sun XY, Wang TT, et al. (2002). Modulation of cyclophilin gene expression by N-4-(hydroxyphenyl) retinamide: association with reactive oxygen species generation and apoptosis. *Mol. Carcinog.* 33: 16-24.
- Javadov SA, Clarke S, Das M, Griffiths EJ, et al. (2003). Ischaemic preconditioning inhibits opening of mitochondrial permeability transition pores in the reperfused rat heart. *J. Physiol.* 549: 513-524.
- Lummis SC, Beene DL, Lee LW, Lester HA, et al. (2005). Cis-trans isomerization at a proline opens the pore of a neurotransmitter-gated ion channel. *Nature* 438: 248-252.
- Nakagawa T, Shimizu S, Watanabe T, Yamaguchi O, et al. (2005). Cyclophilin D-dependent mitochondrial permeability transition regulates some necrotic but not apoptotic cell death. *Nature* 434: 652-658.
- Scorrano L, Ashiya M, Buttke K, Weiler S, et al. (2002). A distinct pathway remodels mitochondrial cristae and mobilizes cytochrome c during apoptosis. *Dev. Cell* 2: 55-67.
- Temkin V, Huang Q, Liu H, Osada H, et al. (2006). Inhibition of ADP/ATP exchange in receptor-interacting protein-mediated necrosis. *Mol. Cell. Biol.* 26: 2215-2225.
- Vyssokikh MY, Katz A, Rueck A, Wuensch C, et al. (2001). Adenine nucleotide translocator isoforms 1 and 2 are differently distributed in the mitochondrial inner membrane and have distinct affinities to cyclophilin D. *Biochem. J.* 358: 349-358.
- Wang X (2001). The expanding role of mitochondria in apoptosis. *Genes Dev.* 15: 2922-2933.
- Woodman CR, Price EM and Laughlin MH (2003). Selected contribution: aging impairs nitric oxide and prostacyclin mediation of endothelium-dependent dilation in soleus feed arteries. *J. Appl. Physiol.* 95: 2164-2170.
- Yasuda O, Fukuo K, Sun X, Nishitani M, et al. (2006). Apop-1, a novel protein inducing cyclophilin D-dependent but Bax/Bak-related channel-independent apoptosis. *J. Biol. Chem.* 281: 23899-23907.